

Disentangled Generation with Information Bottleneck for Few-Shot Learning

Zhuohang Dang, Jihong Wang, Minnan Luo, Chengyou Jia, Caixia Yan, Qinghua Zheng

dangzhuohang@stu.xjtu.edu.cn

Abstract

Few-shot learning (FSL), which aims to classify unseen classes with few samples, is challenging due to data scarcity. Although various generative methods have been explored for FSL, the entangled generation process of these methods exacerbates the distribution shift in FSL, thus greatly limiting the quality of generated samples. To these challenges, we propose a novel Information Bottleneck (IB) based Disentangled Generation Framework for FSL, termed as DisGenIB, that can simultaneously guarantee the discrimination and diversity of generated samples. Specifically, we formulate a novel framework with information bottleneck that applies for both disentangled representation learning and sample generation. Different from existing IB-based methods that can hardly exploit priors, we demonstrate our DisGenIB can effectively utilize priors to further facilitate disentanglement. We further prove in theory that some previous generative and disentanglement methods are special cases of our DisGenIB, which demonstrates the generality of the proposed DisGenIB. Extensive experiments on challenging FSL benchmarks confirm the effectiveness and superiority of DisGenIB, together with the validity of our theoretical analyses. Our codes will be open-source upon acceptance.

Introduction

Few-shot Learning (FSL) that recognizes the unseen classes with few labeled samples is challenging, since models trained with very few samples notoriously lead to underfitting or overfitting problems (Liu, Song, and Qin 2020). There are mainly two routes to address the FSL problem: the algorithm-based methods and the data augmentation-based methods. For the algorithm-based methods (Sun et al. 2019; Liu et al. 2021), researchers try to learn robust task-agnostic feature representations or an effective meta-learner that can quickly adapt models' parameters with few samples. Nonetheless, these methods severely suffer from the intra-class variance of labeled samples, due to the data scarcity of FSL. In this paper, we set our sights on the data augmentation-based methods, which tackle data scarcity in a straightforward way. These methods typically augment data by training generative models on seen classes for fitting data distribution (Li et al. 2020b; Luo et al. 2021), and then utilize the learned knowledge to generate samples on the unseen classes. Some works also introduce external knowledge, *e.g.*, semantics or attributes, as label-related priors to

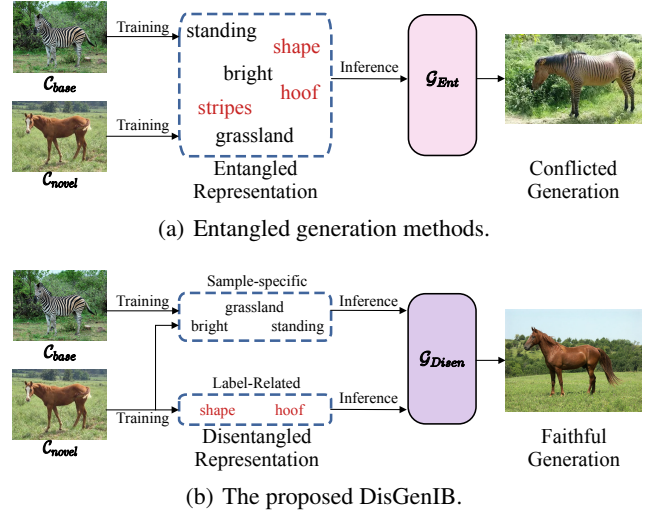


Figure 1: Illustration of unseen sample generation in FSL, where C_{base} and C_{novel} denote classes of seen and unseen; G_{Ent} and G_{Disen} indicate the generator of entangled and disentangled. The red words refer to label-related information, while the black ones denote sample-specific information.

enhance the generation (Xu and Le 2022).

Notably, previous data augmentation-based methods usually fail to disentangle two complementary components: label-related and sample-specific information, which are roughly decomposed from image information. This problem exacerbates the distribution shift between seen and unseen categories in FSL, and thus misleads the generated samples into deviating from true data distribution. Here, the label-related information corresponds to a specific class, inheriting discriminative information for classification. The sample-specific information that characterizes the diversity of samples, *e.g.*, view, light and pose, is independent of labels and generalizable to all classes. As shown in Figure 1(a), the entangled generation process misuses some label-related information (*i.e.*, stripes of zebra) to generate unseen samples (*i.e.*, horse), which leads to conflicted generations. Some methods (Xu et al. 2021b; Cheng et al. 2021) regard features for classification as label-related information to disentangle features. However, according to (Yue et al.

2020), it is infeasible since feature extractors and classifiers fail to obtain comprehensive and accurate label-related features. Thus, it is significantly necessary to develop an effective disentangled generation framework for FSL.

Recently, various methods (Jeon et al. 2021; Pan et al. 2021) have been proposed for disentangled representation learning with Information Bottleneck (IB) (Tishby, Pereira, and Bialek 2000) that can extract label-related information from input. For example, (Pan et al. 2021) employs IB as training objective for the encoder-decoder architecture, which encodes the class-specific information into label-related features for compression, while eliminating discriminative information from sample-specific features for disentanglement. Some downstream tasks, *e.g.*, classification, detection and generation, are followed to evaluate the efficacy of the disentangled representations (Bao 2021; Kim, Lee, and Ro 2021; Uddin et al. 2022). However, these methods rely on a two-stage process for generation, which fails to jointly optimize the representation learning and sample generation for optimality. Moreover, these methods are difficult to utilize the widely used priors in FSL to facilitate the generation of unseen classes.

In this paper, we propose a unified framework for disentangled representation learning and sample generation based on IB, termed as DisGenIB, which can also effectively utilize priors to facilitate disentanglement. As shown in Figure 1(b), our DisGenIB can generate unseen samples with label-related information from the labeled sample and diverse sample-specific information from various samples. The former ensures the discrimination of specific class, while the latter enriches the diversity of generated samples. Since the mutual information involved in IB cannot be optimized directly, we formulate a tight and tractable bound via variational inference. We also prove in theory that disentangled IB (DisenIB) and conditional variational autoencoder (CVAE) are special cases of the proposed DisGenIB, which demonstrate the superiority of DisGenIB on generality. In summary, the contributions of this paper are as follows:

- We propose an IB-based disentangled generation framework to synthesize samples of unseen classes for FSL. It is capable of simultaneously maintaining the discrimination and diversity of generated samples from principle. To the best of our knowledge, this is the first work that explores IB for disentangled generation for FSL.
- In theory, we derive a tight and tractable bound to solve the optimization problem of DisGenIB, and prove that some previous disentanglement and generative methods, including DisenIB, CVAE and AVAE, are special cases of the proposed DisGenIB.
- Extensive experiments demonstrate the significant performance improvement of our DisGenIB, which outperforms the state-of-the-arts by more than 5% and 1% in 5-way 1-shot and 5-shot FSL tasks, respectively.

Related Works

Few-Shot Learning

FSL aims to learn concepts of unseen classes with very few labeled samples, mainly in the following two ways.

(1) Algorithm-based methods that learn a feasible feature space or a meta-learner that can quickly adapt to new tasks with few samples. For example, to learn an effective meta-learner, MAML (Finn, Abbeel, and Levine 2017) effectively learns models with good potential by maximizing the parameters’ sensitivity to the loss of new tasks. To rectify the decision boundaries, EPNet (Rodríguez et al. 2020) utilizes embedding propagation to smooth the manifold. While for the feasible feature space, Prototypical Networks (Snell, Swersky, and Zemel 2017) alleviates the intra-class bias by viewing the feature centroid as class prototype, where new samples can be classified via nearest neighbors. BD-CSPN (Liu, Song, and Qin 2020) rectifies the prototype by assigning pseudo-labels to samples with high confidence. (2) Data augmentation-based methods try to directly generate unseen samples for FSL. AFHN (Li et al. 2020b) generates samples with generative adversarial networks pre-trained on seen classes. There are some methods introducing priors to further improve quality of generated samples. To name a few, R-SVAE (Xu and Le 2022) uses class semantics to formalize a conditional generator with attributes. MM-Res (Pahde et al. 2021) explores multi-modal consistency between images and texts to enrich the diversity of generated samples.

However, with prior or not, these methods fail to achieve the disentanglement during generation process, thus suffering from the distribution shift. In contrast, our DisGenIB provides a unified framework from the information theoretic perspective. Not only can it ensure the disentangled representation learning and sample generation, but also effectively leverages priors, thus simultaneously maintaining the discrimination and diversity of generated samples.

Disentangled Representation Learning

Following the encoder-decoder framework, disentangled representation learning aims to learn mutually independent representations from input. For example, β -VAE (Higgins et al. 2016) learns factorized representations by adjusting the hyperparameter β , which controls the trade-off between reconstruction performance and disentanglement. Causal-VAE (Yang et al. 2021) employs structured causal model to recover the independent latent factors with causal structure. InfoGAN (Chen et al. 2016) learns disentangled representation through maximizing the mutual information between latent factors and observations. Moreover, IB is introduced to disentanglement methods as a regularizer to refine the learned representations (Gao et al. 2021a; Jeon et al. 2021). However, these methods fail to demonstrate the power of disentanglement in principle. In contrast, DisGenIB theoretically analyzes the disentanglement performance, together with proving the conditional variational autoencoder (CVAE) (Sohn, Lee, and Yan 2015) is special case of DisGenIB.

Disentangled Generative Information Bottleneck

Given input sample X with its label Y , let (A, Z) be a pair of disentangled representations of X , where A is the representation of label-related information inherited from X , while

Z encodes the sample-specific information. Variables A and Z are complementary to each other. From an information-theoretic perspective, we propose DisGenIB for disentangled representation learning and sample generation in a unified framework by solving optimization problem

$$\begin{aligned} \max_{A,Z} \mathcal{L}_{DisGenIB} = & \underbrace{I(X; A, Z)}_{\text{Reconstruction}} + \underbrace{I(A; Y) - \beta I(X; A)}_{\text{Compression}} \\ & - \underbrace{(1 + \alpha) I(Y; Z)}_{\text{Disentanglement}}, \end{aligned} \quad (1)$$

where maximizing mutual information $I(X; A, Z)$ encourages disentangled representation pair (A, Z) to be sufficient for input X . Maximizing the second term $I(A; Y) - \beta I(X; A)$ follows traditional IB to find a maximally compressed A of X , which preserves as much as possible the information on Y (Tishby, Pereira, and Bialek 2000). For the third term, minimizing mutual information $I(Y; Z)$ aims to eliminate the label-related information from sample-specific representation Z , so as to acquire disentanglement between variables A and Z . Hyperparameter α and β control the degree of disentanglement and compression, respectively.

Estimation of DisGenIB

Note that mutual information based objective ($\mathcal{L}_{DisGenIB}$) is intractable to directly compute and optimize since mutual information usually consists of integral on high-dimensional data. To this issue, we follow previous work (Alemi et al. 2016), and leverage variational inference to estimate corresponding bounds for three terms. Due to space limitations, the detailed proof is shown in supplementary materials.

Reconstruction term. Let $Q_{\phi_1}(X|A, Z)$ be a variational approximation to true posterior $P(X|A, Z)$ with parameter ϕ_1 , we formulate a tractable lower bound for $I(X; A, Z)$ as

$$\begin{aligned} I(X; A, Z) &= \int P(X, A, Z) \log \frac{P(X|A, Z)}{P(X)} da dx dz \quad (2) \\ &\geq \int P(X, A, Z) \log Q_{\phi_1}(X|A, Z) da dx dz + H(X), \end{aligned}$$

where $H(X)$ is constant that can be ignored.

Compression term. Let $Q_{\gamma}(Y|A)$ be a variational approximation to true posterior $P(Y|A)$ with parameter γ , we derive a tractable lower bound of $I(A; Y)$ as

$$\begin{aligned} I(A; Y) &= \int P(A, Y) \log \frac{P(Y|A)}{P(Y)} da dy \\ &\geq \int P(A, Y) \log Q_{\gamma}(Y|A) da dy + H(Y), \end{aligned}$$

where $H(Y)$ is a constant that can be ignored.

Following the strategy used in (Wang et al. 2021), we use Contrastive Log-ratio Upper Bound (CLUB) (Cheng et al. 2020) as an estimator of mutual information $I(X; A)$, i.e.,

$$\begin{aligned} I(X; A) &\leq I_{v\text{CLUB}}(X; A) = \mathbb{E}_{P(X,A)}[\log Q_{\theta_A}(A|X)] \\ &\quad - \mathbb{E}_{P(X)} \mathbb{E}_{P(A)}[\log Q_{\theta_A}(A|X)], \end{aligned}$$

where variational distribution $Q_{\theta_A}(A|X)$ is an approximation to true posterior $P(A|X)$ with parameter θ_A .

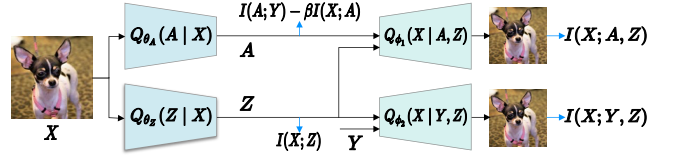


Figure 2: An overview training procedure of DisGenIB, where blue arrows denote corresponding constraints.

Disentanglement term. It is difficult to estimate an upper bound of mutual information $I(Y; Z)$ since the sample-specific representation Z is independent of label variable Y . To this end, we derive in Theorem 1 an equivalent training objective based on Markov chain $Y \leftrightarrow X \leftrightarrow Z$.

Theorem 1. Let X, Y, Z be random variables with joint distribution $P(X, Y, Z)$. Assuming $P(X, Y, Z)$ follows Markov chain $Y \leftrightarrow X \leftrightarrow Z$, i.e., $P(X, Y, Z) = P(X)P(Y|X)P(Z|X)$, we have

$$I(Y; Z) = I(X; Z) + I(X; Y) - I(X; Y, Z), \quad (3)$$

where $I(X; Y)$ is a constant.

Proof. Please see supplementary material for proof.

Similar to the estimation of mutual information $I(X; A)$ and $I(X; A, Z)$ above, the corresponding bounds of $I(X; Z)$ and $I(X; Y, Z)$ can be derived with the help of variational distributions $Q_{\theta_Z}(Z|X)$ and $Q_{\phi_2}(X|Y, Z)$, respectively (see supplementary for detailed proof and derivation).

In summary, we illustrate the overview training procedure of DisGenIB in Figure 2. In detail, $Q_{\theta_Z}(Z|X)$ and $Q_{\theta_A}(A|X)$ parameterized with θ_Z and θ_A can be viewed as two encoders to infer the sample-specific representation Z and label-related representation A from Gaussian distribution of input X . $Q_{\phi_1}(X|A, Z)$ and $Q_{\phi_2}(X|Y, Z)$ parameterized with ϕ_1 and ϕ_2 can be viewed as two decoders to reconstruct input X from the joint distribution $P(A, Z)$ and $P(Y, Z)$, respectively. The last term $Q_{\gamma}(Y|A)$ that is parameterized by γ , can be regarded as a classifier to predict label Y according to the label-related representation A .

Involving priors into DisGenIB

Note that the objective of DisGenIB in Equation (1) is formulated without any priors. In point of fact, there are some available priors of label-related information, such as class semantics, hierarchy and attributes (Li et al. 2020a; Xu and Le 2022). These priors provide critical information of unseen classes to guide the training process of FSL, thereby significantly improving performance. It is therefore reasonable to assume that the label-related information follows priors, which are distributed as $P(A)$.¹ In this sense, we utilize prior distribution $P(A)$ and derive the following Lemma 1 and Theorem 2 for an efficient reduction of the proposed DisGenIB.

¹Note that we don't explore the case where the prior distribution $P(Z)$ is provided, since Z only contains the sample-specific information that is less operational meaning.

Lemma 1. Let Y be label variable, A be variable containing label-related information and Z be variable with sample-specific information. Given prior distribution $P(A)$ of label-related information A , the following inequality holds

$$I(A; Z) \geq I(Y; Z). \quad (4)$$

Proof. Please see supplementary for detailed proof.

Theorem 2. Given prior distribution $P(A)$ and Markov chain $A \leftrightarrow X \leftrightarrow Z$, the optimization problem (1) is reduced to optimization problem

$$\max_Z \mathcal{L}_{DisGenIB}^{Prior} = I(X; A, Z) - \alpha' I(X; Z), \quad (5)$$

where hyperparameter $\alpha' = \frac{1+\alpha}{2+\alpha}$ controls the trade-off between reconstruction and disentanglement.

Proof. With prior distribution $P(A)$, the compression term in Equation (1) turns to be constant C since the values of mutual information $I(X; A)$ and $I(Y; A)$ are determined.

Moreover, according to Lemma 1, we have

$$\begin{aligned} \mathcal{L}_{DisGenIB} &\geq I(X; A, Z) - (1 + \alpha)I(A; Z) + C \\ &= I(X; A, Z) + C \\ &\quad - (1 + \alpha)(I(X; A) + I(X; Z) - I(X; A, Z)) \quad (6) \\ &= (2 + \alpha)I(X; A, Z) - (1 + \alpha)I(X; Z) + C', \quad (7) \end{aligned}$$

where $C' = C - (1 + \alpha)I(X; A)$ is a constant that can be ignored. The derivation of $I(A; Z)$ in Equation (6) holds due to the Theorem 1 and Markov chain $A \leftrightarrow X \leftrightarrow Z$ (Kim and Mnih 2018). With the formulations of α' and $\mathcal{L}_{DisGenIB}^{Prior}$, the proof is completed.

Note that the terms in $\mathcal{L}_{DisGenIB}^{Prior}$ have been estimated using Equation (2) and vCLUB, respectively. Therefore, given prior distribution $P(A)$, the proposed DisGenIB degenerates to an encoder $I(X; Z)$ and a decoder $I(X; A, Z)$, which is evidently more efficient than the case without prior.

Theoretical Analysis

In this section, we demonstrate the generality of DisGenIB in theory that previous disentanglement (Pan et al. 2021) and generative methods (Sohn, Lee, and Yan 2015; Xu et al. 2021b) are special cases of our DisGenIB.

Connection with Disentangled IB

Disentangled IB (DisenIB) (Pan et al. 2021) develops IB principle for optimal disentangled representation learning, by solving the following optimization problem

$$\min_{A, Z} \mathcal{L}_{DisenIB} = -I(A; Y) - I(X; Z, Y) + I(A; Z). \quad (8)$$

Compared to previous disentanglement methods (Nie et al. 2020; Jeon et al. 2021), DisenIB is an effective and interpretable model due to its consistency on maximum compression (Pan et al. 2021). We prove in Theorem 3 that DisenIB is a special case of our DisGenIB, and thus demonstrate the effectiveness of DisGenIB on disentanglement (see supplementary for proof in detail).

Theorem 3. For disentangled representation learning, DisGenIB is reduced to DisenIB when $\alpha = 0$ and $\beta = 1$.

In spite of the similarity, our DisGenIB further overcomes some defects of DisenIB. Note that DisenIB tackles the disentanglement term $I(A; Z)$ via adversarial training with complicated data sampling and rearrangement; Moreover, it is significantly difficult to achieve Nash equilibrium in adversarial training. In contrast, our disentanglement strategy is more effective and stable because the compression and disentanglement terms are optimized directly via reparameterization trick with standard sample batches.

Connection with Conditional Variational Autoencoder (CVAE)

CVAE (Sohn, Lee, and Yan 2015; Verma et al. 2018) is a dominant generative model, which is usually used in FSL to synthesize extra samples of unseen classes based on knowledge of seen classes, such as SVAE (Xu and Le 2022), DCVAE (Zhang et al. 2021b) and VFD (Xu et al. 2021b), etc. It is formulated as solving the following optimization problem

$$\begin{aligned} \max_Z \mathcal{L}_{CVAE} &= \mathbb{E}_{P(X, Y)} \mathbb{E}_{P(Z|X)} [\log Q(X|Z, Y)] \\ &\quad - \beta \mathbb{E}_{P(X)} [D_{KL}(P(Z|X) \| H(Z))], \end{aligned} \quad (9)$$

where D_{KL} refers to KL-divergence; $H(Z)$ denotes the prior distribution of variable Z ; $\mathbb{E}_{P(X, Y)}$ and $\mathbb{E}_{P(X)}$ denote data sampling that can be approximated by sample batches in optimization; hyperparameter β controls the trade-off between reconstruction and disentanglement. We prove in Theorem 4 that CVAE is a special case of our DisGenIB without considering disentangled representation learning.

Theorem 4. For sample generation, DisGenIB is reduced to CVAE when the disentangled representation learning is ignored, i.e., the label-related information A is absolutely provided by label variable Y in $\mathcal{L}_{DisGenIB}$.

Proof. We use Theorem 1 and replace the label-related information A with label variable Y in objective $\mathcal{L}_{DisGenIB}$, arriving at

$$\mathcal{L}_{DisGenIB} = (2 + \alpha)I(X; Y, Z) - (1 + \alpha)I(X; Z) + \bar{C}, \quad (10)$$

where the compression term degenerates to a constant \bar{C} . To solve this optimization problem, we further estimate an upper bound of $I(X; Z)$ by

$$\begin{aligned} I(X; Z) &= \int P(X, Z) \log \frac{P(Z|X)}{P(Z)} dx dz \\ &\leq \int P(X)P(Z|X) \log P(Z|X) dx dz - \int P(Z) \log R(Z) dz \\ &= \mathbb{E}_{P(X)} [D_{KL}(P(Z|X) \| R(Z))], \end{aligned} \quad (11)$$

where $R(Z)$ is a variational approximation to marginal distribution $P(Z)$. The inequality holds due to the non-negativity property of $D_{KL}(P(Z) \| R(Z))$. Additionally, the upper bound of $I(X; Y, Z)$ can be derived by

$$\begin{aligned} I(X; Y, Z) &\geq \int P(X, Y, Z) \log Q_{\phi_2}(X|Y, Z) dx dy dz \\ &= \int P(X, Y)P(Z|X) \log Q_{\phi_2}(X|Y, Z) dx dy dz \\ &= \mathbb{E}_{P(X, Y)} \mathbb{E}_{P(Z|X)} [\log Q_{\phi_2}(X|Y, Z)]. \end{aligned} \quad (12)$$

Method	Using Priors	Backbone	miniImageNet		tieredImageNet	
			5-way 1-shot	5-way 5-shot	5-way 1-shot	5-way 5-shot
CGCS (Gao et al. 2021b)	No	ResNet-12	67.02 ± 0.20%	82.32 ± 0.14%	71.66 ± 0.23%	75.50 ± 0.15%
RENet (Kang et al. 2021)	No	ResNet-12	67.60 ± 0.44%	82.58 ± 0.30%	71.61 ± 0.51%	85.28 ± 0.35%
RFS (Tian et al. 2020)	No	ResNet-12	64.82 ± 0.60%	82.14 ± 0.43%	71.52 ± 0.69%	86.03 ± 0.49%
InvEq (Rizve et al. 2021)	No	ResNet-12	67.28 ± 0.80%	84.78 ± 0.52%	71.87 ± 0.89%	86.82 ± 0.58%
DeepEMD (Zhang et al. 2020)	No	ResNet-12	65.91 ± 0.82%	82.41 ± 0.56%	71.16 ± 0.87%	86.03 ± 0.58%
AFHN (Li et al. 2020b)	No	ResNet-18	62.38 ± 0.72%	78.16 ± 0.56%	-	-
infoPatch (Liu et al. 2021)	No	ResNet-12	67.67 ± 0.45%	82.44 ± 0.31%	71.51 ± 0.52%	85.44 ± 0.35%
FRN (Wertheimer and Tang 2021)	No	ResNet-12	66.45 ± 0.19%	82.83 ± 0.13%	72.06 ± 0.22%	86.89 ± 0.14%
PAL (Ma et al. 2021)	No	ResNet-12	69.37 ± 0.64%	84.40 ± 0.44%	72.25 ± 0.72%	86.95 ± 0.47%
ODE (Xu et al. 2021a)	No	ResNet-12	67.76 ± 0.46%	82.71 ± 0.31%	71.89 ± 0.52%	85.96 ± 0.35%
MeTAL (Baik et al. 2021)	No	ResNet-12	59.64 ± 0.38%	76.20 ± 0.19%	63.89 ± 0.43%	80.14 ± 0.40%
HGNN (Yu et al. 2022)	No	ResNet-12	67.02 ± 0.20%	83.00 ± 0.13%	72.05 ± 0.23%	86.49 ± 0.15%
DisGenIB	No	ResNet-12	76.31 ± 0.84%	85.56 ± 0.53%	76.92 ± 0.90%	87.32 ± 0.59%
TriNet (Chen et al. 2019b)	Yes	ResNet-18	58.12 ± 1.37%	76.92 ± 0.69%	-	-
TRAML (Li et al. 2020a)	Yes	ResNet-12	67.10 ± 0.52%	79.54 ± 0.60%	-	-
TADAM (Xing et al. 2019)	Yes	ResNet-12	65.21 ± 0.30%	75.20 ± 0.27%	69.08 ± 0.47%	82.58 ± 0.31%
FSLKT (Peng et al. 2019)	Yes	ConvNet-128	64.42 ± 0.72%	74.16 ± 0.56%	-	-
MetaDT (Zhang et al. 2022)	Yes	ResNet-12	69.08 ± 0.73%	83.40 ± 0.51%	70.56 ± 0.90%	85.17 ± 0.56%
SVAE (Xu and Le 2022)	Yes	ResNet-12	73.01 ± 0.24%	83.13 ± 0.40%	76.36 ± 0.65%	85.65 ± 0.50%
DisGenIB + Prior	Yes	ResNet-12	79.56 ± 0.81%	86.18 ± 0.52%	77.60 ± 0.89%	87.38 ± 0.58%

Table 1: Comparison with SOTA methods on miniImageNet and tieredImageNet.

According to Equation (11) and (12), the proposed DisGenIB degenerates to the following optimization problem

$$\max_Z \mathbb{E}_{P(X,Y)} \mathbb{E}_{P(Z|X)} [\log Q_{\phi_2}(X|Y, Z)] - \alpha' \mathbb{E}_{P(X)} [D_{KL}(P(Z|X) \| R(Z))], \quad (13)$$

where $\alpha' = \frac{1+\alpha}{2+\alpha}$. Note that the objective in Equation (13) is consistent with CVAE. The proof is completed.

Connection with attribute-based VAE (A-VAE)

Given prior distribution $P(A)$, CVAE defined in Equation (9) turns to attribute-based VAE (A-VAE) (Cheng et al. 2021; Xu and Le 2022), formulated as solving optimization problem

$$\max_Z \mathcal{L}_{A-VAE} = \mathbb{E}_{P(X,A)} \mathbb{E}_{P(Z|X)} [\log Q(X|Z, A)] - \beta \mathbb{E}_{P(X)} [D_{KL}(P(Z|X) \| H(Z))]. \quad (14)$$

In this sense, the generation process is based on priors A instead of label Y . A-VAE can therefore fully leverage priors to generate more faithful samples of unseen classes for FSL (Xu et al. 2021b). We prove in Theorem 5 that A-VAE is a special case of our DisGenIB with prior distribution $P(A)$.

Theorem 5. *For sample generation, DisGenIB is reduced to A-VAE given prior distribution $P(A)$.*

Proof. Given prior distribution $P(A)$, the objective of DisGenIB turns to be $\mathcal{L}_{DisGenIB}^{Prior}$ according to Theorem 2. Similar to the proof in Theorem 4, we get the consistency of two terms in $\mathcal{L}_{DisGenIB}^{Prior}$ and \mathcal{L}_{A-VAE} . The proof is completed.

Note that both CVAE and A-VAE fail to explicitly employ disentangled representation learning for generation. As a result, CVAE struggled in generating samples of unseen classes since their labels Y are hardly available during training, while A-VAE cannot be implemented without priors. In contrast, our DisGenIB with disentangled representation learning relieves the distribution shift in generation, and further takes advantage of priors to facilitate the disentangled generation.

FSL inference with DisGenIB

Problem Definition. The training process of FSL is typically divided into two stages: pre-training and meta-test. In the pre-training phase, a base dataset is given as $\mathcal{D}_{base} = \{(\mathbf{x}_i, y_i) : y_i \in \mathcal{C}_{base}, i = 1, 2, \dots, D\}$ with substantial labeled samples of size D , where \mathcal{C}_{base} refers to the base categories set; $\mathbf{x}_i \in \mathbb{R}^d$ denotes the d -dimensional feature of the i -th sample, associated with a label $y_i \in \mathcal{C}_{base}$. While in the meta-test phase of N -way K -shot FSL tasks, there are two sets sampled from novel category set \mathcal{C}_{novel} ($\mathcal{C}_{base} \cap \mathcal{C}_{novel} = \emptyset$): support set and query set. The support set is defined as $\mathcal{S} = \{(\mathbf{x}_i, y_i) : y_i \in \mathcal{C}_{novel}, i = 1, 2, \dots, N \times K\}$, where N categories are sampled from the novel category set \mathcal{C}_{novel} with K labeled samples for each category. Correspondingly, the query set that is used to evaluate model’s performance is denoted by $\mathcal{Q} = \{(\mathbf{x}_i, y_i) : y_i \in \mathcal{C}_{novel}, i = 1, 2, \dots, N \times M\}$, where M is the number of samples for each category. The main purpose of FSL is to learn an effective classifier for query set \mathcal{Q} over the support set \mathcal{S} as well as the base dataset \mathcal{D}_{base} .

Inference. We train DisGenIB on the base dataset \mathcal{D}_{base} to learn a generative model for synthesizing an additional dataset $\mathcal{S}' = \{(\mathbf{x}_i, y_i) : y_i \in \mathcal{C}_{novel}, i = 1, 2, \dots\}$ with sufficient labeled samples of novel classes \mathcal{C}_{novel} . Specifically, we utilize encoder $Q_{\theta_A}(A|X)$ to sample A from the input, or directly sample from prior distribution $P(A)$ when given priors. To enrich the diversity of generated samples, we utilize the encoder $Q_{\theta_Z}(Z|X)$ to obtain the sample-specific information from $\mathcal{S} \cup \mathcal{Q}$. Then we utilize the decoder $Q_{\phi_1}(X|A, Z)$ to generate samples of \mathcal{S}' , whose labels are assigned by the corresponding label-related information.

Motivated by (Snell, Swersky, and Zemel 2017), we learn a prototypical classifier with the help of DisGenIB and support samples, where prototypes are estimated as the feature centroid of each class. In detail, we have two prototypes \mathbf{p} and \mathbf{p}' that are estimated from \mathcal{S} and \mathcal{S}' , respectively. Similar to (Zhang et al. 2021a), we use Multivariate Gaussian Distribution (MGD) to model the mean and variance of these two prototypes, which are then fused to get the rectified prototype $\hat{\mathbf{p}}$ for evaluation.

Experiments

Experimental Setup

We evaluate DisGenIB on three FSL benchmarks, including miniImageNet, tieredImageNet and CIFAR-FS. Due to the page limit, the implementation and training details are given in supplementary.

Datasets. The miniImageNet and tieredImageNet, *i.e.*, the subsets of ILSVRC-2012 (Deng et al. 2009), are two standard benchmarks for the FSL task. More specifically, miniImageNet contains 100 classes with 600 images of size 84×84 per class, while tieredImageNet includes 608 classes with around 1200 images of size 84×84 per class. The CIFAR-FS benchmark used for FSL is a subset of CIFAR100 (Krizhevsky, Hinton et al. 2009). It contains 100 classes with 600 images of size 32×32 per class. For fair comparison, we follow previous works (Vinyals et al. 2016; Ren et al. 2018; Bertinetto et al. 2018) to split these datasets into training, validation and testing subsets, respectively.

Evaluation Metrics. In meta-testing, we run 5-way 1/5-shot classification tasks on 600 episodes randomly sampled from the test set, where 15 query images are randomly sampled per class for evaluation. For each experiment, we report the mean accuracy and the 95% confidence interval.

Comparison to State-of-the-Art

In this section, we report the results of both our DisGenIB and current SOTA methods on FSL. We divide these SOTA methods into two categories, depending on whether they utilize priors.

Evaluation on miniImageNet and CIFAR-FS. These two datasets have similar structures with randomly partitioned classes. As shown in Table 1 and 2, DisGenIB surpasses SOTA methods by more than 7% in 1-shot tasks without priors. Compared to previous entangled generators AFHN and SVAE, the disentangled generation process of DisGenIB can maintain the discrimination of generated samples and thus

Weight	BackBone	CIFAR-FS	
		1-shot	5-shot
MetaDT (Zhang et al. 2022)	ResNet-12	79.03	88.50
RFS (Tian et al. 2020)	ResNet-12	71.51	86.00
PAL (Ma et al. 2021)	ResNet-12	77.10	88.00
CRF-GNN (Tang et al. 2021)	CovNet-256	76.45	88.42
InvEq (Rizve et al. 2021)	ResNet-12	76.83	89.26
CGCS (Gao et al. 2021b)	ResNet-12	71.66	85.50
MeTAL (Baik et al. 2021)	ResNet-12	67.97	82.17
SCL (Ouali and Hudelot 2021)	ResNet-12	76.50	88.00
RENet (Kang et al. 2021)	ResNet-12	74.51	86.60
SEGA (Yang and Wang 2022)	ResNet-12	78.45	86.00
DisGenIB	ResNet-12	85.19	89.54
DisGenIB + Prior	ResNet-12	86.84	89.76

Table 2: Comparison with SOTA methods on CIFAR-FS.

Proportion	mini	tiered	CIFAR-FS
train	28.15%	5.73%	31.25%
test	70.37%	12.09%	71.43%

Table 3: Proportion of common attributes on different sets.

greatly boosts the performance, *i.e.*, 2%-3%. Other metric-based methods utilize various training strategies to learn robust features, *e.g.*, cross-attention (Kang et al. 2021), feature reconstruction (Wertheimer and Tang 2021) and alignment (Xu et al. 2021a). Unfortunately, due to the entangled learning strategy, these methods inevitably introduce sample-specific noise into the learned features. In contrast, DisGenIB learns disentangled representations to mainly focus on the label-related information, which eliminates the impact of sample-specific information and thus outperforms these methods by 3%-9%. Moreover, when priors are provided, our DisGenIB regards them as prior distribution to further facilitate the disentanglement. In contrast, other methods, *e.g.*, TriNet and TRAML, only treat priors as extra features to rectify the classifier, which fail to fully use the priors. As a result, our DisGenIB exceeds these methods by more than 7%.

Evaluation on tieredImageNet. As shown in Table 1, using priors or not, our DisGenIB is superior to SOTA methods by a large margin, *i.e.*, 1%-5%. Nevertheless, compared to the other two datasets, the performance improvement over tieredImageNet is limited. We infer that this is mainly due to the partition of the dataset. Specifically, tieredImageNet contains much more classes that need to be divided by high-level semantics, which is more challenging since the shared information among different partitions is limited. These issues undermine the generalization of the label-related information extraction $Q(A|X)$ and generation process $Q(X|A, Z)$. To quantitatively verify the above analysis, we report the shared information among different partitions of three datasets, which is evaluated by the proportion of the

Methods	Sim	Methods	Acc
Baseline	0.55	Baseline	52.73
SRestoreNet	0.79	AFHN	62.38
BD-CSPN	0.67	IDeMe-Net	59.14
FSLKT	0.68	VI-Net	61.05
Ours	0.95	Ours	68.36

Table 4: Cosine similarity between the estimated and real prototypes. Here baseline is the original prototype on \mathcal{S} .

Table 5: Classification accuracy of using generated samples with linear classifier. Here baseline is the classifier learned on \mathcal{S} .

common attributes shared by train and test sets. As shown in Table 3, tieredImageNet has notably less common attributes between train and test sets than other two datasets. Thus, the performance over tieredImageNet is vulnerable to being diminished. We will explore this issue in future work.

Ablation Study

To further analyze the effect of each key component, we conduct substantial experiments on miniImageNet in 5-way 1-shot setting. Due to the page limit, more experiments can be found in the supplementary.

Influence of generated samples. The quality of generated samples, *i.e.*, discrimination and diversity, is the key to evaluating the generative models in FSL. To quantitatively study the efficacy of generated samples, we utilize them to rectify the prototype and linear classifiers. The former relies on the discrimination, while the latter depends on both discrimination and diversity of generated samples. To be more convincing, we also present the results of existing SOTA methods, *e.g.* SRestoreNet (Xue and Wang 2020), BD-CSPN (Liu, Song, and Qin 2020) and FSLKT (Peng et al. 2019). **1)** We calculate the average cosine similarity between the rectified prototype \hat{p} and the true prototype over test set. As shown in Table 4, our DisGenIB surpasses these baselines by more than 0.15 over cosine similarity. **2)** We utilize the generated samples as extra samples to learn a linear classifier. As shown in Table 5, the classification accuracy of our DisGenIB exceeds the other three generative methods, *i.e.*, AFHN (Li et al. 2020b), IDeMe-Net (Chen et al. 2019a) and VI-Net (Luo et al. 2021), by more than 6%. These results demonstrate the high discrimination and diversity of samples generated by our DisGenIB, which can effectively alleviate the data scarcity of FSL.

Influence of Regularizers. We propose a novel objective in Equation (1) that consists of the conventional reconstruction term $I(X; A, Z)$, together with some regularization terms that control the disentanglement and compression of A and Z , including $I(A; Y) - \beta I(X; A)$ (*i.e.*, $IB(A; X; Y)$) and $I(Y; Z)$. As shown in Table 6, when removing both terms, the performance drops by around 3% on average, mainly due to insufficient disentanglement on A and Z . When merely using $IB(A; X; Y)$, the performance significantly increases

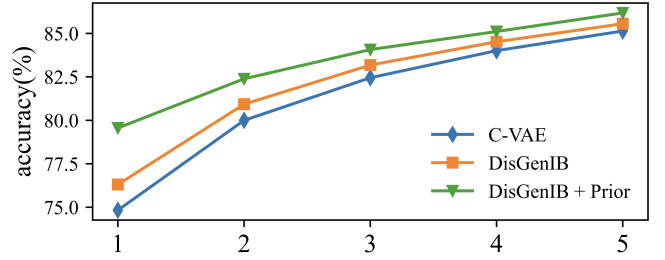


Figure 3: Influence of disentanglement on different number of support samples.

Regularizer		miniImageNet		CIFAR-FS	
$I(Y; Z)$	$IB(A; X; Y)$	5w1s	5w5s	5w1s	5w5s
✓		71.52	84.76	83.13	87.33
	✓	73.95	85.20	84.07	88.56
	✓	75.94	85.31	84.93	88.87
✓	✓	76.31	85.56	85.19	89.54

Table 6: Comparative results of different regularizers on miniImageNet and CIFAR-FS. 5w1s and 5w5s stand for 5-way 1-shot and 5-way 5-shot, respectively.

by around 2% on average. In addition, due to the entanglement of label-related information, the improvement of using only $I(Y; Z)$ is limited since DisGenIB fails to maintain the discrimination of generated samples without $IB(A; X; Y)$. The best performance is achieved when using both terms, demonstrating the effectiveness of the proposed regularizers in disentangling A and Z .

Influence of disentanglement. To study the effectiveness of the disentanglement, we report the results of our DisGenIB without disentanglement, *i.e.*, CVAE. For comparison, we also report results of the original DisGenIB, as well as DisGenIB that uses priors to facilitate disentanglement. As shown in Figure 3, with different numbers of support samples, the best disentangled “DisGenIB + Priors” exceeds the other two methods by a large margin, while the worst disentangled CVAE drops drastically in performance. Thus, the performance is positively related to the degree of disentanglement, which is consistent with the study on regularizers. These results demonstrate the necessity of disentanglement for maintaining the discrimination of generative models.

Conclusion

In this paper, we propose a novel IB-based disentangled generation framework to generate faithful unseen samples for FSL. Specifically, our DisGenIB solves disentangled representation learning and sample generation in a unified framework, together with effectively leveraging priors. Additionally, we theoretically prove that previous disentanglement and generative methods are special cases of our DisGenIB, which demonstrates the generality of DiGenIB. Benefiting from these, our DisGenIB achieves state-of-the-art performance on challenging FSL benchmarks. Our DisGenIB provides a novel and promising perspective on solving FSL

tasks with interpretable information theoretic objectives.

References

- Alemi, A. A.; Fischer, I.; Dillon, J. V.; and Murphy, K. 2016. Deep variational information bottleneck. *arXiv preprint arXiv:1612.00410*.
- Baik, S.; Choi, J.; Kim, H.; Cho, D.; Min, J.; and Lee, K. M. 2021. Meta-Learning with Task-Adaptive Loss Function for Few-Shot Learning. In *Proceedings of the IEEE/CVF International Conference on Computer Vision*, 9465–9474.
- Bao, F. 2021. Disentangled Variational Information Bottleneck for Multiview Representation Learning. In *CAAI International Conference on Artificial Intelligence*, 91–102. Springer.
- Bertinetto, L.; Henriques, J. F.; Torr, P.; and Vedaldi, A. 2018. Meta-learning with differentiable closed-form solvers. In *International Conference on Learning Representations*.
- Chen, X.; Duan, Y.; Houthoofd, R.; Schulman, J.; Sutskever, I.; and Abbeel, P. 2016. Infogan: Interpretable representation learning by information maximizing generative adversarial nets. *Advances in neural information processing systems*.
- Chen, Z.; Fu, Y.; Wang, Y.-X.; Ma, L.; Liu, W.; and Hebert, M. 2019a. Image deformation meta-networks for one-shot learning. In *Proceedings of the IEEE/CVF Conference on Computer Vision and Pattern Recognition*, 8680–8689.
- Chen, Z.; Fu, Y.; Zhang, Y.; Jiang, Y.-G.; Xue, X.; and Sigal, L. 2019b. Multi-level semantic feature augmentation for one-shot learning. 9, 4594–4605. IEEE.
- Cheng, H.; Wang, Y.; Li, H.; Kot, A. C.; and Wen, B. 2021. Disentangled Feature Representation for Few-shot Image Classification. *arXiv preprint arXiv:2109.12548*.
- Cheng, P.; Hao, W.; Dai, S.; Liu, J.; Gan, Z.; and Carin, L. 2020. Club: A contrastive log-ratio upper bound of mutual information. In *International conference on machine learning*, 1779–1788. PMLR.
- Deng, J.; Dong, W.; Socher, R.; Li, L.-J.; Li, K.; and Fei-Fei, L. 2009. Imagenet: A large-scale hierarchical image database. In *Proceedings of the IEEE/CVF Conference on Computer Vision and Pattern Recognition*, 248–255.
- Finn, C.; Abbeel, P.; and Levine, S. 2017. Model-agnostic meta-learning for fast adaptation of deep networks. In *International Conference on Machine Learning*, 1126–1135. PMLR.
- Gao, G.; Huang, H.; Fu, C.; Li, Z.; and He, R. 2021a. Information bottleneck disentanglement for identity swapping. In *Proceedings of the IEEE/CVF conference on computer vision and pattern recognition*, 3404–3413.
- Gao, Z.; Wu, Y.; Jia, Y.; and Harandi, M. 2021b. Curvature Generation in Curved Spaces for Few-Shot Learning. In *Proceedings of the IEEE/CVF International Conference on Computer Vision*, 8691–8700.
- Higgins, I.; Matthey, L.; Pal, A.; Burgess, C.; Glorot, X.; Botvinick, M.; Mohamed, S.; and Lerchner, A. 2016. beta-vae: Learning basic visual concepts with a constrained variational framework. In *International Conference on Learning Representations*.
- Jeon, I.; Lee, W.; Pyeon, M.; and Kim, G. 2021. IB-GAN: Disentangled Representation Learning with Information Bottleneck Generative Adversarial Networks. In *Proceedings of the AAAI Conference on Artificial Intelligence*, 9, 7926–7934.
- Kang, D.; Kwon, H.; Min, J.; and Cho, M. 2021. Relational Embedding for Few-Shot Classification. In *Proceedings of the IEEE/CVF International Conference on Computer Vision*, 8822–8833.
- Kim, H.; and Mnih, A. 2018. Disentangling by factorising. In *International Conference on Machine Learning*, 2649–2658. PMLR.
- Kim, J.; Lee, B.-K.; and Ro, Y. M. 2021. Distilling robust and non-robust features in adversarial examples by information bottleneck. *Advances in Neural Information Processing Systems*, 17148–17159.
- Krizhevsky, A.; Hinton, G.; et al. 2009. Learning multiple layers of features from tiny images. Citeseer.
- Li, A.; Huang, W.; Lan, X.; Feng, J.; Li, Z.; and Wang, L. 2020a. Boosting few-shot learning with adaptive margin loss. In *Proceedings of the IEEE/CVF Conference on computer vision and pattern recognition*, 12576–12584.
- Li, K.; Zhang, Y.; Li, K.; and Fu, Y. 2020b. Adversarial feature hallucination networks for few-shot learning. In *Proceedings of the IEEE/CVF Conference on Computer Vision and Pattern Recognition*, 13470–13479.
- Liu, C.; Fu, Y.; Xu, C.; Yang, S.; Li, J.; Wang, C.; and Zhang, L. 2021. Learning a few-shot embedding model with contrastive learning. In *Proceedings of the AAAI Conference on Artificial Intelligence*, 10, 8635–8643.
- Liu, J.; Song, L.; and Qin, Y. 2020. Prototype rectification for few-shot learning. In *European Conference on Computer Vision*, 741–756. Springer.
- Luo, Q.; Wang, L.; Lv, J.; Xiang, S.; and Pan, C. 2021. Few-shot learning via feature hallucination with variational inference. In *Proceedings of the IEEE/CVF Winter Conference on Applications of Computer Vision*, 3963–3972.
- Ma, J.; Xie, H.; Han, G.; Chang, S.-F.; Galstyan, A.; and Abd-Almageed, W. 2021. Partner-assisted learning for few-shot image classification. In *Proceedings of the IEEE/CVF International Conference on Computer Vision*, 10573–10582.
- Nie, W.; Karras, T.; Garg, A.; Debnath, S.; Patney, A.; Patel, A.; and Anandkumar, A. 2020. Semi-supervised stylegan for disentanglement learning. In *International Conference on Machine Learning*, 7360–7369. PMLR.
- Ouali, Y.; and Hudelot, C. 2021. Spatial contrastive learning for few-shot classification. In *Joint European Conference on Machine Learning and Knowledge Discovery in Databases*, 671–686. Springer.
- Pahde, F.; Puscas, M.; Klein, T.; and Nabi, M. 2021. Multi-modal prototypical networks for few-shot learning. In *Proceedings of the IEEE/CVF Winter Conference on Applications of Computer Vision*, 2644–2653.
- Pan, Z.; Niu, L.; Zhang, J.; and Zhang, L. 2021. Disentangled information bottleneck. In *Proceedings of the AAAI Conference on Artificial Intelligence*, 10, 9285–9293.

- Peng, Z.; Li, Z.; Zhang, J.; Li, Y.; Qi, G.-J.; and Tang, J. 2019. Few-shot image recognition with knowledge transfer. In *Proceedings of the IEEE/CVF International Conference on Computer Vision*, 441–449.
- Ren, M.; Triantafillou, E.; Ravi, S.; Snell, J.; Swersky, K.; Tenenbaum, J. B.; Larochelle, H.; and Zemel, R. S. 2018. Meta-Learning for Semi-Supervised Few-Shot Classification. In *International Conference on Learning Representations*.
- Rizve, M. N.; Khan, S.; Khan, F. S.; and Shah, M. 2021. Exploring complementary strengths of invariant and equivariant representations for few-shot learning. In *Proceedings of the IEEE/CVF Conference on Computer Vision and Pattern Recognition*, 10836–10846.
- Rodríguez, P.; Laradji, I.; Drouin, A.; and Lacoste, A. 2020. Embedding propagation: Smoother manifold for few-shot classification. In *European Conference on Computer Vision*, 121–138. Springer.
- Snell, J.; Swersky, K.; and Zemel, R. 2017. Prototypical networks for few-shot learning.
- Sohn, K.; Lee, H.; and Yan, X. 2015. Learning structured output representation using deep conditional generative models. *Advances in neural information processing systems*.
- Sun, Q.; Liu, Y.; Chua, T.-S.; and Schiele, B. 2019. Meta-transfer learning for few-shot learning. In *Proceedings of the IEEE/CVF Conference on Computer Vision and Pattern Recognition*, 403–412.
- Tang, S.; Chen, D.; Bai, L.; Liu, K.; Ge, Y.; and Ouyang, W. 2021. Mutual crf-gnn for few-shot learning. In *Proceedings of the IEEE/CVF Conference on Computer Vision and Pattern Recognition*, 2329–2339.
- Tian, Y.; Wang, Y.; Krishnan, D.; Tenenbaum, J. B.; and Isola, P. 2020. Rethinking few-shot image classification: a good embedding is all you need? In *European Conference on Computer Vision*, 266–282. Springer.
- Tishby, N.; Pereira, F. C.; and Bialek, W. 2000. The information bottleneck method. *arXiv preprint physics/0004057*.
- Uddin, M. P.; Xiang, Y.; Lu, X.; Yearwood, J.; and Gao, L. 2022. Federated Learning via Disentangled Information Bottleneck. *IEEE Transactions on Services Computing*.
- Verma, V. K.; Arora, G.; Mishra, A.; and Rai, P. 2018. Generalized zero-shot learning via synthesized examples. In *Proceedings of the IEEE conference on computer vision and pattern recognition*, 4281–4289.
- Vinyals, O.; Blundell, C.; Lillicrap, T.; Wierstra, D.; et al. 2016. Matching networks for one shot learning.
- Wang, Z.; Luo, Y.; Qiu, R.; Huang, Z.; and Baktashmotlagh, M. 2021. Learning to diversify for single domain generalization. In *Proceedings of the IEEE/CVF International Conference on Computer Vision*, 834–843.
- Wertheimer, D.; and Tang, L. 2021. Few-shot classification with feature map reconstruction networks. In *Proceedings of the IEEE/CVF Conference on Computer Vision and Pattern Recognition*, 8012–8021.
- Xing, C.; Rostamzadeh, N.; Oreshkin, B.; and O Pinheiro, P. O. 2019. Adaptive cross-modal few-shot learning.
- Xu, C.; Fu, Y.; Liu, C.; Wang, C.; Li, J.; Huang, F.; Zhang, L.; and Xue, X. 2021a. Learning dynamic alignment via meta-filter for few-shot learning. In *Proceedings of the IEEE/CVF Conference on Computer Vision and Pattern Recognition*, 5182–5191.
- Xu, J.; and Le, H. 2022. Generating Representative Samples for Few-Shot Classification. In *Proceedings of the IEEE/CVF Conference on Computer Vision and Pattern Recognition*, 9003–9013.
- Xu, J.; Le, H.; Huang, M.; Athar, S.; and Samaras, D. 2021b. Variational feature disentangling for fine-grained few-shot classification. In *Proceedings of the IEEE/CVF International Conference on Computer Vision*, 8812–8821.
- Xue, W.; and Wang, W. 2020. One-shot image classification by learning to restore prototypes. In *Proceedings of the AAAI Conference on Artificial Intelligence*, 04, 6558–6565.
- Yang, F.; and Wang, R. 2022. SEGA: semantic guided attention on visual prototype for few-shot learning. In *Proceedings of the IEEE/CVF Winter Conference on Applications of Computer Vision*, 1056–1066.
- Yang, M.; Liu, F.; Chen, Z.; Shen, X.; Hao, J.; and Wang, J. 2021. CausalVAE: Disentangled representation learning via neural structural causal models. In *Proceedings of the IEEE/CVF Conference on Computer Vision and Pattern Recognition*, 9593–9602.
- Yu, T.; He, S.; Song, Y.-Z.; and Xiang, T. 2022. Hybrid Graph Neural Networks for Few-Shot Learning. In *Proceedings of the AAAI Conference on Artificial Intelligence*, 3, 3179–3187.
- Yue, Z.; Zhang, H.; Sun, Q.; and Hua, X.-S. 2020. Interventional few-shot learning. *Advances in neural information processing systems*, 2734–2746.
- Zhang, B.; Jiang, H.; Li, X.; Feng, S.; Ye, Y.; and Ye, R. 2022. MetaDT: Meta Decision Tree for Interpretable Few-Shot Learning.
- Zhang, B.; Li, X.; Ye, Y.; Huang, Z.; and Zhang, L. 2021a. Prototype completion with primitive knowledge for few-shot learning. In *Proceedings of the IEEE/CVF Conference on Computer Vision and Pattern Recognition*, 3754–3762.
- Zhang, C.; Cai, Y.; Lin, G.; and Shen, C. 2020. Deepemd: Few-shot image classification with differentiable earth mover’s distance and structured classifiers. In *Proceedings of the IEEE/CVF Conference on Computer Vision and Pattern Recognition*, 12203–12213.
- Zhang, Y.; Huang, S.; Peng, X.; and Yang, D. 2021b. Dizygotic Conditional Variational AutoEncoder for Multi-Modal and Partial Modality Absent Few-Shot Learning. *arXiv preprint arXiv:2106.14467*.